Food Hydrocolloids Vol.7 no.3 pp.213–226, 1993

A mixed system composed of different molecular weights konjac glucomannan and kappa carrageenan: large deformation and dynamic viscoelastic study

Kaoru Kohyama, Hiroki Iida[1] and Katsuyoshi Nishinari[2]

National Food Research Institute, 2-1-2 Kannondai, Tsukuba, Ibaraki 305, [1]*San-Ei Gen F.F.I., Inc., 1-11 Sanwa-cho, 1-chome, Toyonaka, Osaka 561, Japan*

[2]*Present address: Faculty of Human Life Science, Osaka City University, Sumiyoshi, Osaka 558, Japan*

Abstract. Rheological properties of mixed gels of konjac glucomannan (KGM) of four different molecular weights with kappa-carrageenan (CAR) were studied by dynamic viscoelastic measurements and tensile testing. Both storage and loss moduli for sol and gel state mixtures containing higher molecular weight KGM were highest. However variation in molecular weight of KGM produced little effect on the gel-to-sol and sol-to-gel transition temperatures of the mixtures. Two systems containing KGM of lower molecular weights showed almost the same stress–strain curves in tensile testing. The breaking stress and the breaking strain for mixed gels became larger with increasing molecular weight of KGM, and the difference was larger than that observed in the dynamic viscoelasticity measurements. It was suggested that weak junction zones are created by the addition of KGM and that the number of weak junction zones and the contour length of flexible chains connecting these weak junction zones increase with increasing molecular weight of KGM.

Introduction

Konjac glucomannan (KGM) is a main component of the tuber of *Amorphophallus konjac* K. Koch and forms a thermally stable gel (Konnyaku) upon addition of an alkaline coagulant. KGM has been utilized as a raw material in the food and polymer industries in Japan since ancient times. It has also been used as a food additive recently in Western countries. KGM shows an interaction with other hydrocolloids (1) and most studies in the Western literature have been devoted to a binary system, such as a mixture of KGM with either carrageenan (2,3) or xanthan gum (4–6).

Generally, rheological properties of gels depend on the molecular structure of the gelling agent. It is known that the number of ionic groups, or degree of substitution in polysaccharides such as agar–agar (7), carrageenan (8,9) or pectin (10) markedly affects gel properties. Relationships between rigidity of gels and molecular weight, which is indexed by the intrinsic viscosity (11), have been studied for gelatin (12,13), alginate (11), carrageenan (14,15), and agarose (16). In mixed systems the gel properties were also affected by the structural change of one component (17–20). Mitchell (21) summarized the molecular weight dependence of the rheological properties of gels: the elastic modulus is independent of molecular weight above a certain limiting value, whilst the rupture strength continues to rise with increasing molecular weight. Since KGM is virtually a neutral polysaccharide and has few acetyl groups, ionic effects on various KGM molecules may be small. However the molecular weight is expected to affect the gel properties.

We obtained four fractions of KGM with different molecular weights and investigated the rheological properties of mixed gels of KGM with kappa-carrageenan (CAR) by dynamic viscoelastic measurements and by tensile testing.

Materials and methods

Materials

Powdered KGM from konjac tuber (cv. Harunakuro) and three fractions of KGM with different molecular weights, prepared by an enzymatic degradation, were kindly supplied by Shimizu Chemical Co. (Hiroshima, Japan). The native KGM (ND) was treated with an enzyme (SP-249, Novo Nordisk A/S, Copenhagen, Denmark) for different reaction times at ambient temperature, and LM3, LM2 and LM1 fractions with low molecular weights were obtained.

A commercially available CAR (San-Ei Gen F.F.I., Inc., Osaka, Japan) was washed with ethanol and then air-dried. Molecular weight was determined as 4.3×10^5 in 50 mmol/dm^3 $NaNO_3$ by gel permeation chromatography (GPC) at room temperature. All chemicals used in this study were of reagent grade.

Chemical analysis

The ratio of mannose (Man) to glucose (Glc) for KGM samples was determined by HPLC. KGM (2 g) was hydrolysed in 2% hydrochloric acid (100 ml) at 100°C for 2 h. After neutralization the solution was diluted to 200 ml and filtrated. The filtrate (20 ml) was again diluted with water up to 50 ml. An aliquot of the solution (20 μl) was applied to the HPLC columns of SUGAR SP1010 and Ionpak KS801 (8 mmID × 30 cm, each) (Showa Denko, Tokyo, Japan) heated at 80°C. Eluent was water with a flow rate of 0.8 ml/min. Man/Glc ratio was calculated from the peak areas of mannose and glucose detected with a refractive index detector Shodex R1 SE-51 (Showa Denko, Tokyo, Japan). Sulfate content was calculated by a gravimetric method (22) after acid decomposition. Analysis of metal ions was carried out using an Inductively Coupled Argon Plasma Emission Spectrophotometer (ICP-AES) (ICAP-575 Mark II, Nippon Jarrell-Ash, Kyoto, Japan).

Molecular weight of KGM

KGM samples were dissolved in cadoxen (23) with stirring for 12 h at room temperature. The cadoxen contained 28% w/w ethylenediamine, 0.35 mol/dm^3 sodium hydroxide, and 1.83% w/w cadmium by atomic absorption spectrophotometry (AA-781, Nippon Jarrel-Ash). Both the KGM solutions and the cadoxen solvent were diluted with the same volume of water and filtered through a glass filter before measurement. Intrinsic viscosities were measured at 25°C using an Ubbelohde viscometer. The flow time for the solvent, diluted cadoxen, was 259 s. Molecular weight of each KGM fraction was determined by GPC at room temperature.

Dynamic viscoelasticity

Powders of KGM and CAR were mixed in the ratio of 1:1 and dispersed in deionized water with agitation at 85°C for 30 min. The total saccharide content was adjusted to 1.5% w/w in dry bases. CAR solution of 1.5 and 0.75% w/w were also prepared. The hot mixture was injected into a cell of a Rheolograph Sol (Toyoseiki Seisakusho, Tokyo) (24,25), which had been heated previously to 75°C. The surface of the sample was covered with silicone oil in order to prevent drying. The temperature was lowered from 75 to 20°C at 1.0°C/min and then heated to 60°C at the same rate with a thermo-module controlled by a microcomputer. The sample sol was subjected to 1 Hz sinusoidal shear oscillations with an amplitude 25 μm corresponding to a shear strain of 0.025. The storage and loss moduli (G′ and G″) were recorded every 1°C.

Tensile testing

The hot mixture of KGM and CAR prepared as described above were poured into moulds to a depth, d, of 11 mm and then covered with glass plates. They were allowed to stand at 25°C for 15 h. The gel was then cut into rings which had an inner diameter R_i of 20 mm and the outer diameter R_o of 30 mm using coaxial cylinders made of stainless steel. Tensile testing of gels was carried out using a Rheoner RE-33005 (Yamaden Co. Ltd, Tokyo) with a 2 kg load cell at 25°C. A ring-shaped gel sample was hung on two polyacetal bars of 7 mm diameter arranged vertically. The gel ring was initially deformed under its own weight and then vertically elongated at the rate of 5 mm/sec. Breaking stress, τ_B, of gels was calculated from the load value, F_B, at a breaking point divided by the initial cross-sectional area, A_0, $= (R_o - R_i)d$ (110 mm^2) of the gel. Breaking strain γ_B was determined as the ratio of the elongation ($2\Delta L$) at a breaking point, to the initial effective circumference C_e (26).

$$C_e = \pi (R_b + R_a)/2 + 2L_0,$$

where R_b; the diameter of the bar (7 mm), R_a; the outer diameter of the hung gel $= R_o - R_i + R_b$ (17 mm), and L_0; the initial distance of two bars (depending on the samples). The dimensions of a sample gel are illustrated in Figure 1. Young's modulus was defined as the slope of each stress–strain curve at small strain range ($\gamma < 0.05$). The measurement was repeated more than 20 times, and the mean value and standard deviation were determined.

Results and discussion

Chemical analysis

Chemical analysis data are shown in Table I. CAR used in the present study contained 22% w/w sulfate groups which was higher than that for CAR (19% w/w) reported previously (9). Since carrageenan containing lower sulfate content forms gels with higher elastic modulus, CAR used in the present work is expected to form less rigid gels. The ratio of mannose to glucose was ~2.0 for all

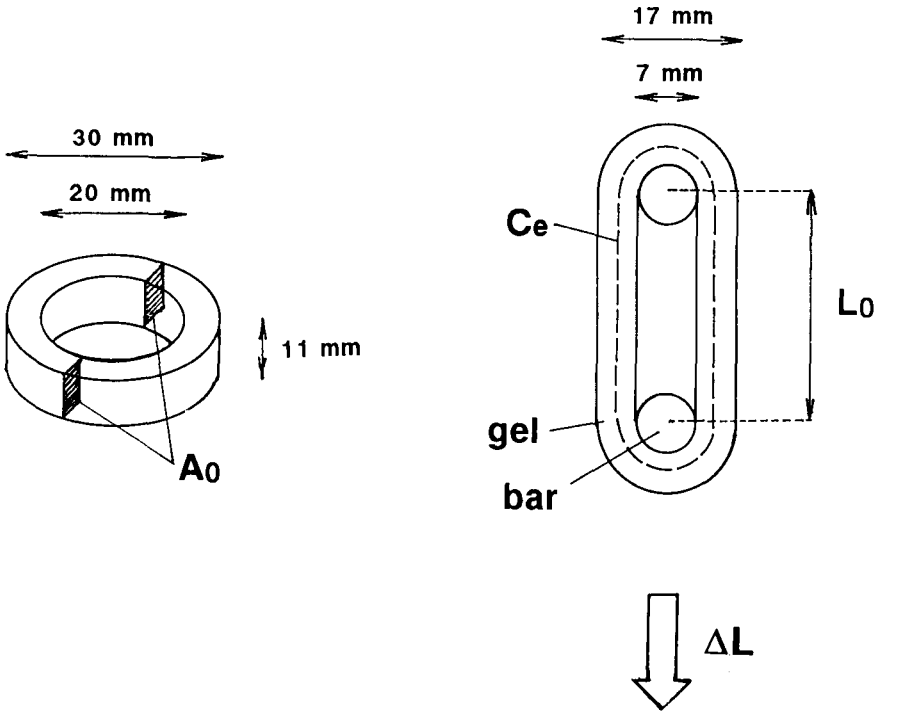

Fig. 1. Shape and dimension of the gel ring for tensile testing.

Table I. Analytical data for polysaccharides

Sample	Man/Glc	Na^+ (μg/g)	K^+ (μg/g)	Ca^{2+} (μg/g)	Fe^{+2} (μg/g)	Mg^{+2} (μg/g)	SO_4^{-2} (%w/w)
CAR	–	3940	80500	21000	60	1010	22.33
KGM-LM1	2.04	8	275	538	–	30	–
KGM-LM2	2.09	6	407	606	–	35	–
KGM-LM3	2.04	7	420	510	–	48	–
KGM-ND*	1.95	6	1185	480	12	50	–

*Non-degraded.

the four KGM fractions, which was higher than 1.6 reported previously (27–30). It was rather close to the ratio 2.1 for glucomannan from Scotch pine (30). However it did not differ significantly before and after the enzyme treatment. This fact supports the statement that KGM does not have any block structures of mannose or glucose (27,28) because it is expected that glucose and mannose residues in glucomannan show the difference in enzyme reactivity. The contents of cations in KGMs were low enough compared with those in CAR as shown in Table I, such that they had little or no effect on the gel properties of CAR, even though it is well known that monovalent (31) or divalent (32) cations affect the elastic modulus of CAR.

Table II. Intrinsic viscosity [η], Huggins' coefficient k′ and molecular weight M_w for various KGM samples

Sample	[η][a] (dL/g)	k′[a]	M_w[b]
LM1	1.98	0.38	2.56×10^5
LM2	2.63	0.31	4.38
LM3	3.50	0.41	5.96
ND	3.91	0.48	6.89

[a]Measurement by Ubbelohde viscometer at 25°C in cadoxen.
[b]Measurement by GPC at room temperature in cadoxen.

All four fractions of KGM were similar in chemical composition. Since there might be a specific structure easily attacked by the enzyme, it may be possible that the higher molecular weight fractions have a different sugar sequence from the lower molecular weight fractions. A chemical study before and after the enzyme treatment would be necessary to confirm this. However it would be very difficult to show that the chemical structures for KGM with different molecular weights are completely the same.

Molecular weight of KGM

Information about the molecular weight is shown in Table II. It is clear that all the four fractions have different molecular weights. KGM lost solubility in water by strong hydrogen bonds like cellulose once it has been purified or dried. Therefore, it was very difficult to make aqueous solutions of pure KGM. We tried to dissolve the KGM in water, but failed. Though it was partially dissolved, the residue was considered to include the KGM with higher molecular weight more than the KGM dissolved in the solution. Because, generally speaking, polymers which have lower molecular weights show higher solubilities. We measured the intrinsic viscosity of aqueous and 4 mol/dm^3 urea solutions of KGM after removing the residue. Values of intrinsic viscosity were found to be arranged in the order expected, i.e. fractions considered to have larger molecular weights showed larger intrinsic viscosities in both solvent systems (data not shown). However the Huggins' coefficients (33) for many cases became >1. This suggests that the solutions were not completely molecularly dispersed and some aggregation occurred in the solutions. Kishida *et al.* (34) also failed to prepare aqueous solution of KGM; they modified KGM by methylation to dissolve in water. Since we wanted to discuss effects of molecular weight the molecular weight needed to be determined correctly. We concluded that water was not an appropriate solvent, and dissolved KGM in cadoxen. The solvent is known to dissolve cellulose and to make a clear, colorless and stable solution (23). As shown in the third column of Table II, reasonable values (0.3–0.5) of Huggins' coefficient were obtained. Intrinsic viscosity increased in the order of LM1, LM2, LM3, and non-degraded sample (ND). The highest value 3.91 dl/g of the intrinsic viscosity in cadoxen at 25°C was much smaller than those reported—4.6–18.8 dl/g for methyl KGM (34) and 7.3–7.7 dl/g for sonicated

KGM (35) in water at 30°C. Weight average molecular weight (M_w, the fourth column of Table II) for four KGMs was also arranged in the same order. The molecular weight value 6.89×10^5 for ND sample was smaller than that for methyl KGM (usually >1 000 000) (34), however it was larger than 4.9×10^5 for two konjac flours determined recently (35). Therefore, the KGM sample was considered not to be significantly damaged by the strong alkalinity of cadoxen. The four fractions of KGM have definitely different molecular weights.

Only four points are not sufficient to derive a relationship between M_w and intrinsic viscosity (η); however, we made a double logarithmic plot of M_w against (η) to confirm whether cadoxen dissolves KGM or not. A linear relationship was obtained as shown in Figure 2. The Mark–Houwink relationship, $(\eta) = K \cdot M_w^a$, was found to be valid, and two parameters K and a were found to be 3.55×10^{-4} dl/g and 0.69 respectively ($r = 0.991$). The a value 0.69 was in the range from 0.5 (Flory θ-solvent) to 0.8 (a thermodynamically good solvent) (36), and was somewhat smaller than 0.74 reported for aqueous methyl KGM by Kishida *et al.* (34). The measured K value was far smaller than that of 6.37×10^{-4} dl/g reported by Kishida *et al.* (34). The Mark–Houwink parameters were near those obtained for guar gum (galactomannan) in water ($K = 3.8 \times 10^{-4}$ dl/g, and $a = 0.723$) as reported by Robinson *et al.* (37). The KGM in cadoxen appears to be more flexible than methyl KGM in water. Clegg *et al.* (35) found that viscosity average molecular mass (M_v), calculated using Kishida *et al.*'s values of K and a for two KGM samples, became lower than those experimentally obtained by GPC and laser light scattering. Shatwell *et al.* (6) argued that methylation may have modified the KGM chain causing extension and a smaller K value like 3.8×10^{-4} dl/g for guar gum gave better M_v for native KGM.

Dynamic viscoelasticity

Cooling curves and heating curves of dynamic viscoelasticity measurements for CAR and mixtures of CAR and KGM are shown in Figures 3 and 4 respectively. All the samples tested were sols at higher temperatures. Both storage and loss moduli for the sol state mixtures at 60°C containing higher molecular weight KGM were highest as shown in Table III. The loss modulus was almost the same

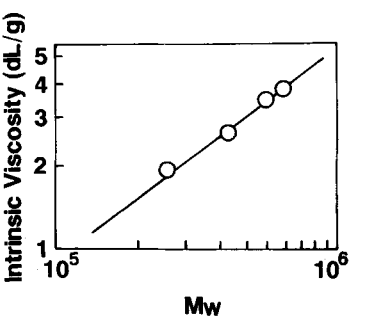

Fig. 2. Double logarithmic plot for intrinsic viscosity versus molecular weight for KGM samples measured in cadoxen at 25°C.

as, or somewhat larger than, the storage modulus as shown in the 6th and 7th columns of Table III. Both moduli increased gradually with decreasing temperature, and then increased steeply at ~30°C. Below this temperature samples lost fluidity and the storage modulus became more than five times larger than the loss modulus at 25°C for all the samples, as shown in the 4th and 5th columns of Table III. Gel state mixtures containing higher molecular weight KGM at 25°C showed larger values in both moduli, except for the mixture containing KGM of the highest molecular weight which showed smaller increases in G′ and G″ at lower temperatures. Gelling or sol-to-gel transition temperature (T_{gel}) was determined as the temperature at which the storage modulus began to deviate from the baseline in the cooling process. Usually the value for the storage modulus was ~2 Pa at T_{gel} as observed in a 1% mixture of

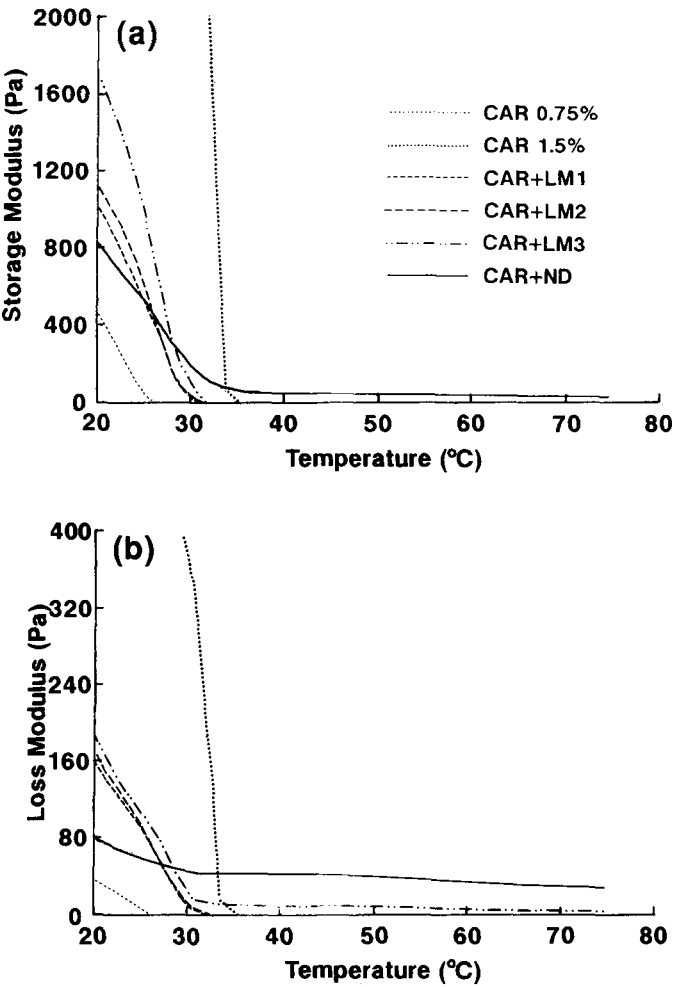

Fig. 3. Temperature dependence of storage (a) and loss (b) moduli for CAR and KGM mixtures in the cooling process. Total polysaccharide content, 1.5% w/w. Cooling rate, 1°C/min.

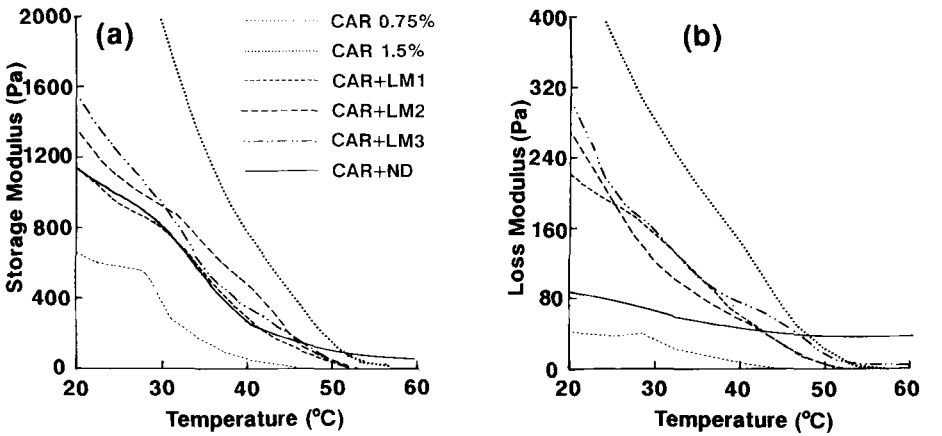

Fig. 4. Temperature dependence of storage (a) and loss (b) moduli for CAR and KGM mixtures in the heating process. Total polysaccharide content, 1.5% w/w. Heating rate, 1°C/min.

Table III. Dynamic viscoelastic characteristics for CAR and KGM mixtures

Sample	T_{gel} (°C)	T_{sol} (°C)	G′25* (Pa)	G″25 (Pa)	G′60 (Pa)	G″60* (Pa)
CAR 1.5%	34	55	4135	680	0.3	0.5
CAR 0.75%	27	43	46	8	0.2	0.0
CAR + LM1	30	50	533	91	0.5	1.2
CAR + LM2	30	49	610	95	0.7	1.3
CAR + LM3	30	50	1010	118	3.8	6.8
CAR + ND	32	53	527	57	38.1	34.7

* G′25 and G″60 represent the storage modulus at 25°C and the loss modulus at 60°C in the cooling process, respectively.

CAR and galactomannan (38). All four systems showed a similar gelling temperature, which was between the gelling temperatures of 1.5 and 0.75% CAR.

The storage and loss moduli for 1.5% CAR gel changed abruptly at ~29°C in the cooling process. The change could not be attributed to the structure breakdown but should be attributed to the slip induced by syneresis (39). Since no such change in shear modulus was observed for mixed systems of CAR and KGM, KGM prevented the syneresis of CAR gel. Even though syneresis occurred, 1.5% CAR gel showed much larger shear moduli than any mixed systems.

When the gel was heated the storage and loss moduli decreased with increasing temperature; however the values were larger than those observed in the cooling process at the same temperature in the temperature range 20–60°C. Melting temperature or gel-to-sol transition temperature (T_{sol}) was defined as the temperature at which the storage modulus in the heating process reached the same level (baseline) as observed in the cooling process. Therefore, samples show similar values of storage and loss moduli as those in the cooling process at a temperature above T_{sol}. As observed for T_{gel}, all four mixed systems showed a similar T_{sol}, which was higher than that for 0.75% CAR and lower than that for

1.5% CAR alone. The difference in molecular weight of KGM had little observable effect on both T_{gel} and T_{sol}. T_{sol} was ~20°C higher than T_{gel} for all the samples. CAR showed thermal hysteresis in temperature scanning measurements of calorimetry (9,32,40), optical rotation (41–46), viscosity (45), conductivity (45) and Cotton–Mouton constant in magnetic birefringence (45). The observed hysteresis in gel formation of the mixed system with KGM was influenced by those characteristics of CAR. A similar hysteresis was also reported for the CAR–galactomannan mixed system (38). Higher T_{sol} than T_{gel} is commonly observed for many thermoreversible gels such as agarose (47–50) and gelatin (51).

Recently a zipper model approach has been proposed to explain the thermoreversible gel-to-sol transition (52). The gel-to-sol transition was treated as an opening process of molecular zippers which make junction zones. According to this approach the heat capacity of gels is written as a function of the number of zippers N, the number of parallel links N in a single zipper, the rotational freedom G of a link, and the energy ϵ required to open a link. An endothermic peak accompanying gel-to-sol transition in a heating curve of differential scanning calorimetry (DSC), as well as an exothermic peak accompanying sol-to-gel transition in a cooling DSC curve, is equivalent to the maximum of the heat capacity. When the temperature is raised from a lower temperature than T_{gel}, G would start from the lower value G_g corresponding to the gel state. Then the gel will expand, which will give rise to an increase in the rotational freedom. On the contrary, when the temperature is lowered from higher temperatures than T_{sol} G will start from the higher value G_s corresponding to the sol state. Therefore the opening of molecular zippers begins to occur at small G values in the heating process while gelation by cooling will take place with decreasing G which starts from large G values at higher temperatures. Then the average effective value of G is small in heating and is large in cooling. As a first approximation, therefore, we can say that T_{sol} is determined by certain average $\bar{G}_g$ of G for gel state and T_{gel} is determined by an average $\bar{G}_s$ of G for sol state. Apparently, $\bar{G}_g < \bar{G}_s$, hence, T_{sol} is expected to be higher than T_{gel}.

In heating the transition caused by the opening of the zippers will start as soon as the temperature arrives at (the tail of the C–T curve corresponding to) $G = G_g$. In cooling, on the contrary, the pair-wise coupling cannot start so easily because of the difficulty for a long molecule in finding its partner in appropriate positions for the zipper construction. Hence a state like supercooling may take place during the cooling process. It is therefore reasonable that the transition is sharper in cooling than in heating, as is observed. This above-mentioned interpretation corresponds well to the experimental fact that the storage modulus G' decreased gradually with increasing temperature (Figure 4), whilst G' began to rise steeply at a narrow temperature region with lowering temperature (Figure 3).

Large-deformation properties

Force–deformation curves and tensile characteristics for gels are shown in

Figure 5 and Table IV respectively. CAR gels are firm and brittle as shown by a large Young's modulus and a small breaking strain. The addition of KGM to CAR made the breaking strain larger. Two systems containing KGM of lower molecular weights (LM1 and LM2) showed almost the same properties in the tensile testing. The breaking stress and the breaking strain for mixed gels of higher molecular weight KGM were larger. Therefore it is considered that KGM of higher molecular weight contributes to formation of a strong network structure in the mixed system. Polymers with high molecular weight can form a network whose junction zones are connected by molecular chains with long contour length. Such a network has enough flexibility and is considered to endure against a strong force or a large deformation. KGM molecules with higher molecular weight have long chains, and produce the rubber-like properties in the gel.

The Young's modulus for CAR with non-degraded KGM (ND) became smaller than that of the other mixed gels, which is consistent with the results of the dynamic viscoelasticity at 25°C. Probably it is influenced by air bubbles in the gel. Since the sol of an ND sample showed an extremely large viscosity, and it was difficult to remove small air bubbles in the mixed sol formed with CAR by either suction or centrifugation. The effect of large molecular weight KGM on breaking stress and breaking strain was very strong, the breaking properties

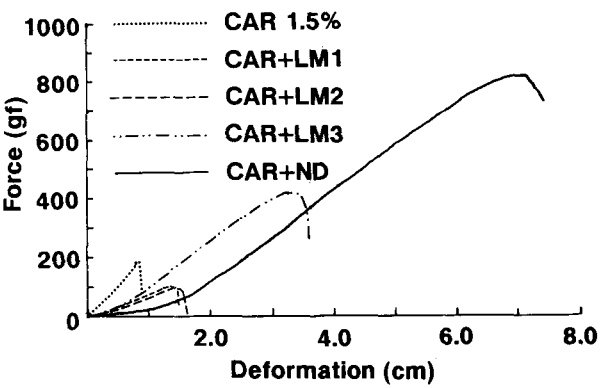

Fig. 5. Force–deformation curves in tensile testing for CAR–KGM mixed gels of 1.5%.

Table IV. Tensile characteristics for mixed gels of CAR and various KGM samples. Total saccharide content: 1.5%

Sample	Breaking stress (kPa)	Breaking strain (cm/cm)	Young's modulus (kPa)
CAR	16.47 ± 2.54	0.210 ± 0.025	60.64 ± 2.04
CAR + LM1	8.57 ± 0.97	0.388 ± 0.043	15.15 ± 1.43
CAR + LM2	9.23 ± 0.84	0.369 ± 0.030	15.46 ± 1.24
CAR + LM3	37.36 ± 1.18	0.870 ± 0.048	20.76 ± 1.09
CAR + ND	74.66 ± 4.55	1.958 ± 0.103	9.97 ± 0.96

Mean ± standard deviation from more than 20 measurements.

became larger than those for other mixtures even though air bubbles decreased these properties. With the exception of the CAR–ND gels, the dynamic viscoelasticity and the Young's modulus in tensile testing increased with molecular weight of KGM among the three mixed gels of CAR and KGM. The difference was smaller than that observed in the breaking properties. The breaking stress greatly increased with increasing molecular weight of KGM in CAR–KGM mixed gels.

Network structure of CAR-KGM

Cairns *et al.* (2) observed no interaction between CAR and KGM from X-ray fibre diffraction patterns for a 1:1 mixture. Then they proposed a model involving CAR network containing the KGM within the CAR gel (2,3) for the mixed gel. According to this model junction zones made from the interaction between CAR and KGM did not exist. Junction zones in the mixed gels were formed only by CAR molecules.

In the present work the structure of a junction zone was independent of the molecular weight of KGM, since gel-to-sol and sol-to-gel transition of the systems occurred at almost the same temperature. As shown in Table III, T_{gel} and T_{sol} for mixed systems were higher than those for the 0.75% CAR gel. Since mixed systems contained 0.75% CAR, the gel structure was stabilized by addition of KGM. However those temperatures for the mixtures were lower than those for 1.5% CAR. Therefore, the interaction between KGM and CAR is weaker than that between CAR and CAR, but strong enough to produce another elastically active chain (53–55). In other words, KGM creates weak junction zones which contribute to rheolgoical characteristics but not to thermal stability.

It is well known that gelatin gels with higher molecular weights melt at higher temperature (56). Molecular weight dependence of melting temperature for methyl cellulose gels was not remarkable even though the molecular weight ranged from 5.1×10^4 to 1.1×10^6 (57).

Since a KGM molecule has few branching points (29), it is essentially a string like cellulose. Therefore, the higher the molecular weight, the longer the KGM chain. The number of weak junction zones N is considered to increase with increasing molecular weight of KGM because Young's modulus and G′ at 25°C for mixed gels increased with increasing molecular weight of KGM (53–55). If the molecular weight of KGM increases, the number N of parallel links in a zipper or the contour length of flexible chains which connect zippers will increase. Since the gel-to-sol and sol-to-gel transition temperatures were almost independent of the molecular weight of KGM, the binding energy ϵ and the rotational freedom G of a parallel link are also considered to be independent of the molecular weight of KGM.

The contour length of flexible chains which connect junction zones is considered to increase because breaking stress and breaking strain increased with the increasing molecular weight of KGM. In conclusion, the increase in molecular weight of KGM increases the number of weak junction zones and

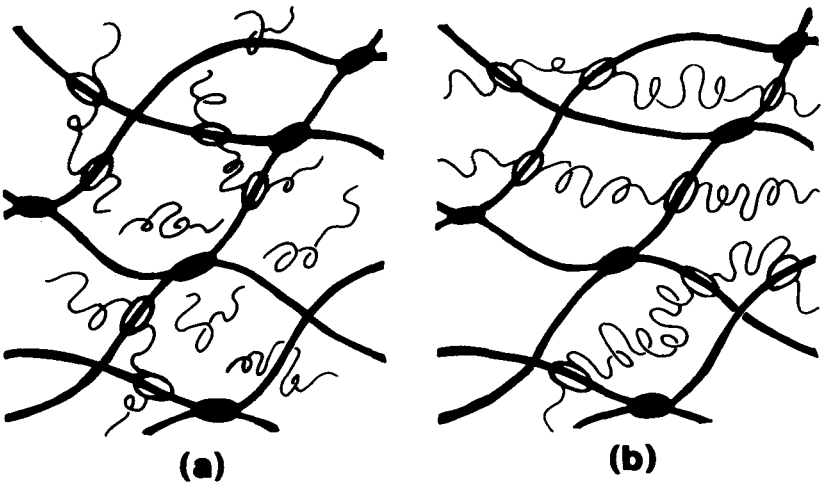

Fig. 6. The effect of the molecular weight of KGM on the gel network structure. Mixed gels of CAR and low molecular weight KGM (a), and CAR and high molecular weight KGM (b). Thick lines represent CAR molecular chains whilst thin lines show KGM chains. The number of elastically active chains and the contour length of active chains increase with increasing molecular weight of KGM. ●, junction zones made by CAR–CAR; ○, weak junction zones made by CAR–KGM.

makes the contour length of flexible chains which connect junction zones longer. As is seen from zipper model approach, T_{gel} or T_{sol} does not shift to higher temperatures with the increasing number of junction zones (zippers). The contour length of flexible chains does not affect T_{gel} or T_{sol} because these temperatures are determined mainly by the structure of junction zones. The effect of the molecular weight increase of KGM on the gel network is schematically shown in Figure 6.

A large error is generally observed in Young's modulus obtained from a stress–strain curve in a large deformation measurement (11), because of the difficulty in determining the tangent. In the present study accuracy in the determination of Young's modulus is unfortunately not high. Measurement of small deformation properties of the gels should be carried out to clarify the structure of the junction zones. It is difficult to define gel-to-sol or sol-to-gel transition temperature of the system more precisely than ±1°C from the dynamic viscoelasticity as a function of temperature. For such a purpose thermal analysis would probably produce better results. Further study, including some small deformation rheology measurements and differential scanning calorimetry for the same systems, is now being undertaken.

Acknowledgement

The authors wish to thank S.Ohashi and T.Ochi of San-Ei Gen F.F.I., Inc. for their kind support. They are indebted to H.Tomizawa of Tosoh Corporation Tokyo Research Center for GPC measurement and A.Yasui of NFRI for cadmium analysis. They also thank Professor K.Kato of Gifu University for discussion concerning the chemical structure of KGM.

References

1. Nishinari,K., Williams,P.A. and Phillips,G.O. (1992) *Food Hydrocoll.*, **6**, 199–222.
2. Cairns,P., Miles,M.J. and Morris,V.J. (1988) *Carbohydr. Polym.*, **8**, 99–104.
3. Cairns,P., Atkins,E.D.T., Miles,M.J. and Morris,V.J. (1991) *Int. J. Biol. Macromol.*, **13**, 65–68.
4. Brownsey,G.J., Cairns,P., Miles,M.J. and Morris,V.J. (1988) *Carbohydr. Res.*, **176**, 329–334.
5. Williams,P.A., Day,D.H., Langdon,M.J., Phillips,G.O. and Nishinari,K. (1991) *Food Hydrocoll.*, **4**, 489–493.
6. Shatwell,K.P., Sutherland,I.W., Ross-Murphy,S.B. and Dea,I.C.M. (1991) *Carbohydr. Polym.*, **14**, 131–147.
7. Nishinari,K. and Watase,M. (1983) *Carbohydr. Polym.*, **3**, 39–52.
8. Watase,M. and Nishinari,K. (1981) *J. Texture Stud.*, **12**, 447–456.
9. Watase,M. and Nishinari,K. (1987) *Makromol. Chem.*, **188**, 2213–2221.
10. Powell,D.A., Morris,E.R., Gidley,M.J. and Rees,D.A. (1982) *J. Mol. Biol.*, **155**, 517–531.
11. Mitchell,J.R. (1979) In Blanshard,J.M.V. and Mitchell,J.R. (eds), *Polysaccharides in Food*, Butterworths, London, pp. 51–72.
12. Ferry,J.D. (1948) *J. Am. Chem. Soc.*, **70**, 2244–2249.
13. Saunders,P.R. and Ward,A.G. (1955) *Nature*, **176**, 26.
14. Ainsworth,P.A. and Blanshard,J.M.V. (1979) *J. Food Technol.*, **14**, 141–147.
15. Rochas,C., Rinaudo,M. and Landry,S. (1990) *Carbohydr. Polym.*, **12**, 255–266.
16. Watase,M. and Nishinari,K. (1983) *Rheol. Acta*, **22**, 580–587.
17. Dea,I.C.M., Morris,E.R., Rees,D.A., Welsh,E.J., Barnes,H.A. and Price,J. (1977) *Carbohydr. Res.*, **57**, 249–272.
18. Ainsworth,P.A. and Blanshard,J.M.V. (1980) *J. Texture Stud.*, **11**, 149–162.
19. Fernandes,P.B., Gonçalves,M.P. and Doublier,J.L. (1991) *Carbohydr. Polym.*, **16**, 253–274.
20. Turquois,T., Rochas,C. and Taravel,F.R. (1992) *Carbohydr. Polym.*, **17**, 263–271.
21. Mitchell,J.R. (1980) *J. Texture Stud.*, **11**, 315–337.
22. Association of Official Analytical Chemists (1990) In Helrich,K. (ed.), *Official Methods of Analysis, 15th edn.* Association of Official Analytical Chemists Inc., Arlington, VA, pp. 688–689.
23. Henley,D. (1961) *Arkiv Kemi*, **18**, 327–392.
24. Kaibara,M. and Fukada,E. (1976) *Thromb. Res.*, **8**, 49–58.
25. Yoshida,M., Kohyama,K. and Nishinari,K. (1992) *Biosci. Biotech. Biochem.*, **56**, 725–728.
26. Tschoegl,N.W., Rinde,J.A. and Smith,T.L. (1970) *J. Sci. Food Agric.*, **21**, 65–70.
27. Kato,K. and Matsuda,K. (1969) *Agric. Biol. Chem.*, **33**, 1446–1453.
28. Shimahara,H., Suzuki,H., Sugiyama,N. and Nisizawa,K. (1975) *Agric. Biol. Chem.*, **39**, 301–312.
29. Maeda,M., Shimahara,H. and Sugiyama,N. (1980) *Agric. Biol. Chem.*, **44**, 245–252.
30. Chanzy,H.D., Grosrenaud,A., Joseleau,J.P., Dube,M. and Marchessault,R.H. (1982) *Biopolymers*, **21**, 301–319.
31. Watase,M. and Nishinari,K. (1982) *Colloid & Polym. Sci.*, **260**, 971–975.
32. Watase,M. and Nishinari,K. (1986) In Phillips,G.O., Wedlock,D.J. and Williams,P.A. (eds), *Gums and Stabilisers for the Food Industry 3*, Elsevier Applied Science Publishers, London and New York, pp. 185–194.
33. Huggins,M.L. (1942) *J. Am. Chem. Soc.*, **64**, 2716–2718.
34. Kishida,N., Okimasu,S. and Kamata,T. (1978) *Agric. Biol. Chem.*, **42**, 1645–1650.
35. Clegg,S.M., Phillips,G.O. and Williams,P.A. (1990) In Phillips,G.O., Wedlock,D.J. and Williams,P.A. (eds), *Gums and Stabilisers for the Food Industry 5*, IRL Press, Oxford, pp. 463–471.
36. Sperling,L.H. (1986) In *Introduction to Physical Polymer Science*, John Wiley & Sons, New York, pp. 81–83.
37. Robinson,G., Ross-Murphy,S.B. and Morris,E.R. (1982) *Carbohydr. Res.*, **107**, 17–32.
38. Fernandes,F.B., Gonçalves,M.P. and Doublier,J.L. (1992) *Carbohydr. Polym.*, **19**, 261–269.
39. Stainsby,G., Ring,S.G. and Chilvers,G.R. (1984) *J. Texture Stud.*, **15**, 23–32.
40. Gekko,K., Mugishima,H. and Koga,S. (1987) *Int. J. Biol. Macromol.*, **9**, 146–152.
41. Dea,I.C.M., McKinnon,A.A. and Rees,D.A. (1972) *J. Mol. Biol.*, **68**, 153–172.
42. Morris,E.R., Rees,D.A. and Robinson,G. (1980) *J. Mol. Biol.*, **138**, 349–362.
43. Rochas,C. and Rinaudo,M. (1980) *Biopolymers*, **19**, 1675–1687.
44. Norton,I.T., Morris,E.R. and Rees,D.A. (1984) *Carbohydr. Res.*, **134**, 89–101.
45. Rochas,C. and Rinaudo,M. (1984) *Biopolymers*, **23**, 735–745.

46. Plashchina,I.G., Muratalieva,I.R., Braudo,E.E. and Tolstoguzov,V.B. (1986) *Carbohydr. Polym.*, **6**, 15–34.
47. Hayashi,A., Kinoshita,K. and Kuwano,M. (1975) *Polymer J.*, **9**, 219–225.
48. Indovina,P.L., Tettamanti,E., Micciancio-Giammarinaro,M.S. and Palma,M.U. (1979) *J. Chem. Phys.*, **70**, 2841–2847.
49. Watase,M. and Nishinari,K. (1987) *Makromol. Chem.*, **188**, 1177–1186.
50. Watase,M., Nishinari,K., Clark,A.H. and Ross-Murphy,S.B. (1989) *Macromolecules*, **22**, 1196–1201.
51. Djabourov,M., Leblond,J. and Papon,P. (1988) *J. Phys. France*, **49**, 319–332.
52. Nishinari,K., Koide,S., Williams,P.A. and Phillips,G.O. (1990) *J. Phys. France*, **51**, 1759–1768.
53. Nishinari,K., Koide,S. and Ogino,K. (1985) *J. Phys. France*, **46**, 793–797.
54. Clark,A.H. and Ross-Murphy,S.B. (1985) *Br. Polym. J.*, **17**, 164–168.
55. Treloar,L.R.G. (1975) In *The Physics of Rubber Elasticity*, 3rd Edition. Clarendon Press, Oxford, pp. 59–79.
56. Eldridge,J.E. and Ferry,J.D. (1954) *J. Phys. Chem.*, **58**, 992–996.
57. Kato,T., Yokoyama,M. and Takahashi,A. (1978) *Coll. Polym. Sci.*, **256**, 15–21.

Received on March 17, 1993; accepted on May 4, 1993